

# Anion Exchange Membranes for Hydrogen Technologies: Challenges and Progress

Xingyu Wu<sup>a</sup> and Xile Hu<sup>§\*ab</sup>

<sup>§</sup>Green & Sustainable Chemistry Award 2022

**Abstract:** Anion exchange membrane fuel cells (AEMFCs) are considered one of the most promising and efficient hydrogen conversion technologies due to their ability to use cost-effective materials. However, AEMFCs are still in an early stage of development and the lack of suitable anion exchange membranes (AEMs) is one major obstacle. In this review, we highlight three major challenges in AEMs development and discuss recent scientific advancements that address these challenges. We identify current trends and provide a perspective on future development of AEMs.

**Keywords:** Anion exchange membranes (AEM) · Anion exchange membrane fuel cells (AEMFC) · Polyelectrolytes



**Dr. Xingyu Wu** is director of research and development at NovaMea SA and scientific specialist in anion exchange membranes (AEMs). He obtained his PhD in Chemistry and Chemical Engineering from Ecole Polytechnique Fédérale de Lausanne (EPFL) in 2023 under the supervision of Prof. Xile Hu. He has spent the last 5 years working on the design and development of anion exchange membranes (AEMs). He is

interested in Green Technologies and Innovations, with a specific focus on the applications of AEMs in hydrogen fuel cells and water electrolyzers.



**Prof. Xile Hu** is Professor of Chemistry at Ecole Polytechnique Fédérale de Lausanne (EPFL). He obtained his PhD from University of California, San Diego and conducted a postdoc study at the California Institute of Technology. He joined EPFL as a tenure-track assistant professor in 2007 and was promoted to associate professor in 2013 and full professor in 2016. His research interests include base-metal catalyzed organic synthesis, artificial enzymes, biocatalysis, electrochemical water splitting and CO<sub>2</sub> reduction, fuel cell catalysis, as well as anion exchange membrane-based energy devices.

ized organic synthesis, artificial enzymes, biocatalysis, electrochemical water splitting and CO<sub>2</sub> reduction, fuel cell catalysis, as well as anion exchange membrane-based energy devices.

## 1. Introduction

The European Union has set a target to reduce greenhouse gas emissions by at least 55% by 2030 and achieve carbon neutrality by 2050.<sup>[1]</sup> The transportation sector contributes approximately one fifth of total CO<sub>2</sub> emissions.<sup>[2]</sup> Hydrogen fuel cells are a promising alternative to conventional internal combustion engines including zero CO<sub>2</sub> emissions, higher efficiency (>60%) while providing similar refueling times (<5 min) and driving ranges

(>500 km).<sup>[3]</sup> The Hydrogen Roadmap for Europe anticipates to power more than 50 million fuel cell vehicles by 2050.<sup>[4]</sup>

Proton exchange membrane fuel cells (PEMFCs) have been utilized in fuel cell vehicles, but their cost competitiveness is hindered by several factors. These include the reliance on expensive platinum-group metals (PGMs) catalysts, graphite/titanium bipolar plates, and Nafion membranes, primarily due to the acidic working environment. These cost-intensive components contribute to the overall high cost of PEMFCs.<sup>[3]</sup> Anion exchange membrane fuel cells (AEMFCs) offer a cost-effective alternative to PEMFCs. By transitioning from an acidic to an alkaline environment (Fig. 1), AEMFCs can employ more affordable catalysts based on Earth-abundant metals, stainless steel bipolar plates, and hydrocarbon-based anion exchange membranes (AEMs). Despite the cost advantage of AEMFCs, their development is still in the early stages. A key obstacle in AEMFCs is the limited availability of durable AEMs with sufficient OH<sup>-</sup> conductivity.

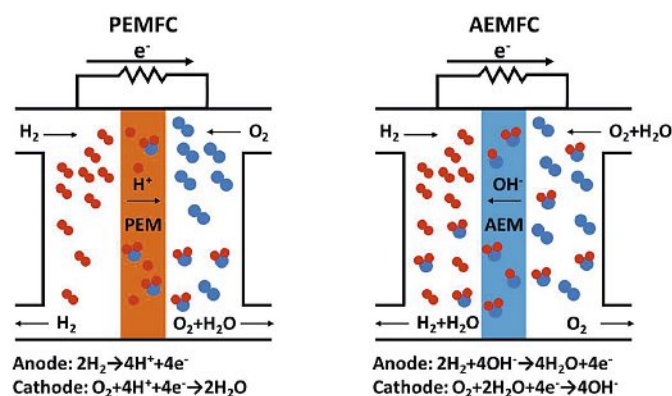


Fig. 1. Schemes of PEMFCs and AEMFCs.

\*Correspondence: Prof. Dr. X. Hu<sup>ab</sup>, E-mail: xile.hu@epfl.ch; Dr. X. Wu, E-mail: novamea.wu@gmail.com,

<sup>a</sup>NovaMea SA, Renens, CH-1020, Switzerland; <sup>b</sup>Institute of Chemical Sciences and Engineering, Ecole Polytechnique Fédérale de Lausanne (EPFL), Lausanne, CH-1015, Switzerland

## 2. Challenges in AEMs

Anion-exchange membranes (AEMs) play a critical role in AEMFCs as they serve both as carriers for  $\text{OH}^-$  ions and barriers to prevent shortcuts and  $\text{H}_2/\text{O}_2$  mixing. AEMs are typically made from polymers containing cationic groups capable of transporting  $\text{OH}^-$  ions. These cationic functional groups can be directly attached to the polymer backbone or connected through long alkyl or aromatic side chains. In some cases, they can be an integral part of the backbone structure. AEMs should simultaneously possess high conductivity ( $>100 \text{ mS cm}^{-1}$  @  $80^\circ\text{C}$ ), excellent chemical stability ( $>1000 \text{ h}$  in  $1 \text{ M KOH}$  @  $80^\circ\text{C}$ ), good mechanical strength ( $>50 \text{ MPa}$ ), limited swelling ( $<30\%$ ), low  $\text{H}_2$  permeability ( $<25 \text{ nmol cm}^{-2} \text{ s}^{-1}$ ) and cost-effectiveness. To make desirable AEMs, three primary scientific challenges must be identified and addressed.

### 2.1 Low Conductivity

The first challenge relates to the inherent low conductivity of AEMs. For instance, Nafion membranes exhibit high proton ( $\text{H}^+$ ) conductivity of up to  $150 \text{ mS cm}^{-1}$  at  $80^\circ\text{C}$ .<sup>[5,6]</sup> In contrast, AEMs derived from Nafion precursors (Fig. 2) typically demonstrate  $\text{OH}^-$  conductivity of less than  $50 \text{ mS cm}^{-1}$  under the same conditions.<sup>[7,8]</sup> This discrepancy arises from the higher molecular weight (17 vs 1) and lower mobility ( $6\pm 1\times 10^{-5} \text{ cm}^2 \text{ s}^{-1}$  vs  $10\pm 2\times 10^{-5} \text{ cm}^2 \text{ s}^{-1}$ ) of conductive  $\text{OH}^-$  ions compared to  $\text{H}^+$  ions in proton exchange membranes (PEMs).

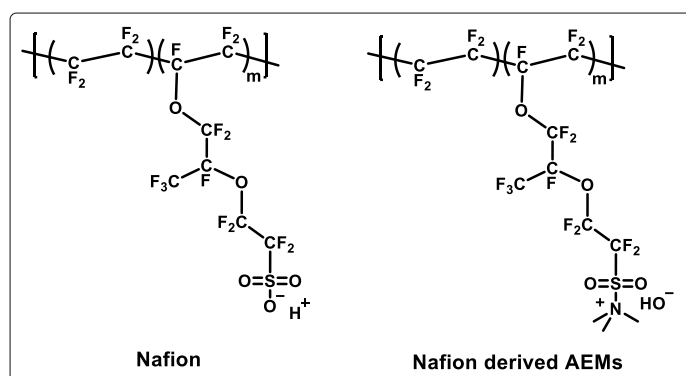


Fig. 2. Structures of Nafion and Nafion-derived AEMs.

### 2.2 Poor Chemical Stability

AEMs face more severe degradation compared to PEMs due to the alkaline working environment, especially at elevated temperature. Various cations, including ammonium, imidazolium, phosphonium, sulfonium, and organic-metal groups, have been tested under alkaline conditions (Fig. 3). However, only a few of them have demonstrated sufficient chemical stability. Additionally, commercially available polyaromatics, such as poly(ether-ether ketone) (PEEK), polysulfone (PSF), and poly(phenylene oxide) (PPO), which contain aryl-ether groups, are susceptible to attack by  $\text{OH}^-$ , leading to polymer chain cleavage (Fig. 3). More importantly, AEMs are prone to undergo more severe degradation by the presence of highly destructive species such as  $\text{HO}$  and  $\text{HO}_2$  radicals, which could be generated on the electrodes and inside the membrane during the operation of AEMFCs.<sup>[9–11]</sup> This chemical degradation often involves the decomposition or detachment of cations and/or the cleavage of the polymer backbone. Consequently, it can result in reduced ion conductivity, loss of mechanical stability, and even fuel cell failure. Overcoming these degradation challenges is crucial for improving the durability and performance of AEMs in AEMFCs.

### 2.3 Trade-off Limitation

The third challenge is the trade-off limitation between conductivity and dimension stability of AEMs. The conductivity of AEMs is primarily determined by the ion-exchange capacity (IEC). Higher IEC typically leads to higher conductivity but it also results in increased water uptake and swelling ratio, which can compromise the dimensional and mechanical stability of AEMs.<sup>[12,13]</sup>

## 3. Current Progress on AEMs

Years of research on anion exchange membranes (AEMs) have led to the discovery of various strategies aimed at addressing the challenges mentioned earlier. Notably, significant progress has been made in resolving the issue of conductivity, with some state-of-the-art AEMs exhibiting conductivities comparable to those of Nafion membranes. The challenges of chemical stability and trade-off limitations have emerged as dominant concerns in the development of desirable AEMs. Consequently, extensive efforts have been dedicated to addressing these challenges. A summary of recent progress towards these three challenges would be valuable for understanding and developing desirable AEMs.

### 3.1 Conductivity

Increasing the ion exchange capacity (IEC) is a highly effective strategy for improving conductivity in AEMs. To achieve the desired conductivity, AEMs typically possess an IEC higher than  $2 \text{ meq. g}^{-1}$ . For instance, He *et al.*<sup>[14]</sup> observed that a poly(2,6-dimethyl-1,4-phenylene oxide) (PPO) AEM with an IEC of  $1.4 \text{ meq. g}^{-1}$  exhibited an  $\text{OH}^-$  conductivity of only  $12.9 \text{ mS cm}^{-1}$  at  $25^\circ\text{C}$ . However, by increasing the IEC to  $2.1 \text{ meq. g}^{-1}$ , the  $\text{OH}^-$  conductivity increased to  $53 \text{ mS cm}^{-1}$ . Furthermore, Mandal *et al.*<sup>[15]</sup> achieved a record-high IEC of  $3.84 \text{ meq. g}^{-1}$  in a poly(butyl norbornene-*b*-bromobutyl norbornene-*b*-butyl norbornene-*b*-bromobutyl norbornene) AEM. This AEM demonstrated a remarkable conductivity of  $212 \text{ mS cm}^{-1}$  at  $80^\circ\text{C}$ , surpassing the benchmark Nafion membrane ( $150 \text{ mS cm}^{-1}$ ) under the same conditions.

When tested in fuel cells, AEMFCs utilizing these high-conductivity AEMs exhibited comparable peak power density to Nafion-based PEMFCs. For example, the QAPPT AEM developed by Peng *et al.*<sup>[16]</sup> demonstrated a conductivity of  $116 \text{ mS cm}^{-1}$  at  $80^\circ\text{C}$ , and AEMFCs using this AEM achieved a peak power density of  $1500 \text{ mW cm}^{-2}$ . Similarly, the GT82-15 AEM fabricated by Mandal *et al.*<sup>[15]</sup> exhibited a conductivity of  $147 \text{ mS cm}^{-1}$  at  $80^\circ\text{C}$ , and AEMFCs employing this AEM achieved an unprecedented peak power density of  $3500 \text{ mW cm}^{-2}$ , the highest recorded to date. These results highlight the significance of increasing IEC in AEMs to enhance their conductivity and enable high-performance AEMFCs.

### 3.2 Chemical Stability

AEMs comprise of polymer backbones, immobilized cationic groups, and free anions (usually  $\text{OH}^-$ ) that balance the charge. By designing durable and chemically resistant polymer backbones, as well as selecting robust cationic groups, it is possible to improve the overall chemical stability of AEMs.

#### 3.2.1 Cations

Tetramethyl ammonium (TMA) is the simplest cation and has sufficient chemical stability (half-life time  $t_{1/2} = 62 \text{ h}$ ) under strong alkaline solution ( $6 \text{ M KOH}$ ) at  $80^\circ\text{C}$ .<sup>[17]</sup> While attached to polymer backbones, benzylic or alkyl linkages have to be introduced (Fig. 4). Notably, the half-life time of benzylic trimethyl ammonium decreased to  $4.2 \text{ h}$  using the same testing method. This decrease can be attributed to the activation of  $\alpha$ -H acidity by both the benzene ring and the ammonium. Replacing the benzylic linkage with alkyl chains ( $>4$  carbon atoms) can improve the alkaline stability. For instance, alkyl trimethyl ammonium cations with 12

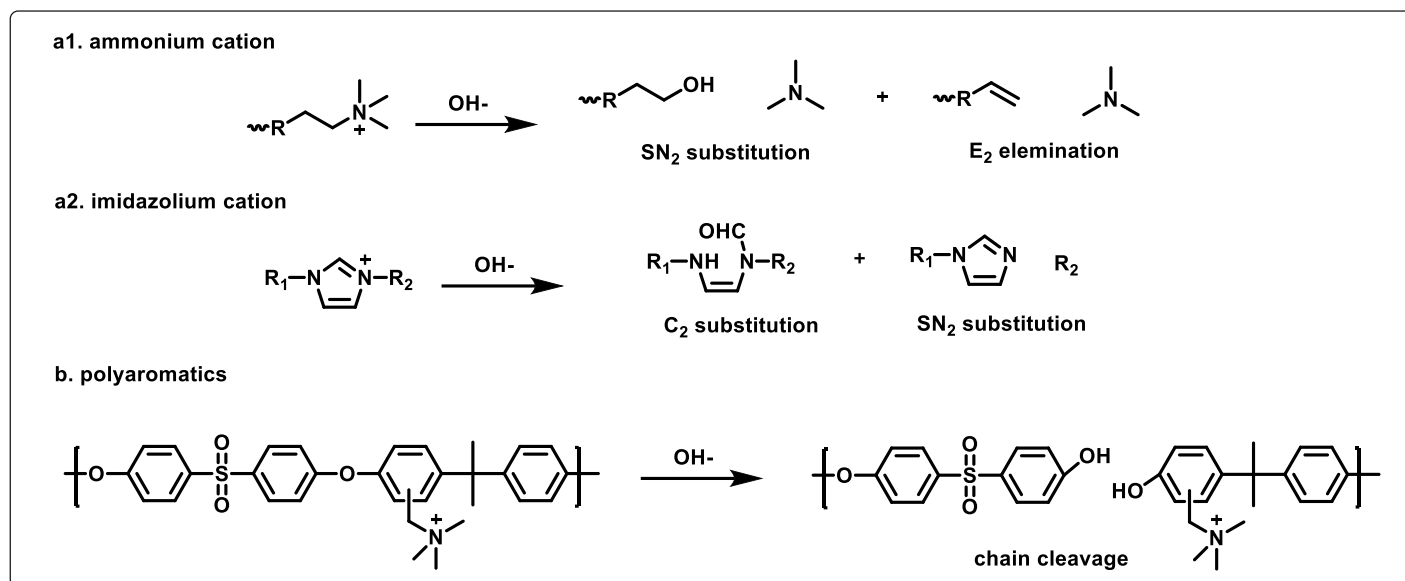


Fig. 3. Degradation mechanisms of typical cations and polyaromatics.

carbon atoms only degrade 11% in 2 M KOH solution at 80 °C for 30 days.<sup>[18]</sup>

In 2015, Marino *et al.*<sup>[17]</sup> conducted a comprehensive investigation into the chemical stability of 26 different quaternary ammonium cations in 6 M NaOH at 160 °C. Among these cations, N-heterocyclic 6-azonia-spiro[5.5]undecanium (ASU) and N,N-dimethyl piperidinium (DMP) demonstrated the highest chemical stability. The half-life times of ASU and DMP were 110 h and 87.3 h, respectively, surpassing that of TMA (61.9 h). The exceptional chemical stability of ASU and DMP can be attributed to the increased transition state energy of both substitution and elimination degradation reactions, which is caused by the minimal ring strain and conformational constraints imposed by their 6-member ring structures.<sup>[19,20]</sup>

Imidazolium cations have been extensively investigated due to the additional chemical stability provided by the resonance effect of the heterocycle. Imidazolium cations with a hydrogen at the C2 position (BMIm) can completely decompose *via* imidazolium ring-opening reactions over 720 h in 1 M KOH at 80 °C (Fig. 3). However, replacing C-H with methyl or phenyl groups and N-CH<sub>3</sub> with butyl or isopropyl groups enhances the stability of imidazolium cations. Imidazolium cations with N1 = N3 = n-butyl, C2 = 1,3,5-trimethyl phenyl, and C1 = C5 = phenyl (Mes-dBIm) have been reported to exhibit exceptional stability (half-life time  $t_{1/2}$  >10000 h) in 3 M NaOD/D<sub>2</sub>O/CD<sub>3</sub>OD at 80 °C.

Phosphonium cations (such as trialkyl phosphonium, triphenyl phosphonium, benzyl triphenyl phosphonium) were unstable in the presence of OH<sup>-</sup> even at room temperature. They can rapidly de-

grade into phosphine oxide *via* the Cahours-Hofmann reaction.<sup>[21]</sup> Yan *et al.*<sup>[22,23]</sup> reported a relatively stable benzyl tris(2,4,6-trimethoxyphenyl)phosphonium cation (BTTP-(p-Me)). The additional methoxy groups offered both electron-donating stabilization and extra steric hindrance. However, spectroscopic studies revealed that these bulky phosphonium cations can still degrade by more than 10% after 1000 h immersion in 1 M KOH at 80 °C.

Organometallic cations, such as cobaltocenium cations,<sup>[24,25]</sup> bis(terpyridine)ruthenium(II) cations,<sup>[26]</sup> and K<sup>+</sup>-complexing crown ether cations,<sup>[27]</sup> show good chemical stability through rational design of complexing ligands. However, their synthesis processes are usually complex.

### 3.2.2 Polymer Backbones

Commercial aryl-ether polyaromatics, such as polysulfone (PSF),<sup>[28]</sup> poly(2,6-dimethyl-1,4-phenylene oxide) (PPO),<sup>[29]</sup> are initially applied to develop AEMs owing to their low-cost, ease of processing and good mechanical properties. However, these AEMs usually showed poor chemical stability due to the backbone cleavage (Fig. 3).<sup>[30]</sup>

Polyethylenes (Fig. 5) are more stable than aryl-ether polyaromatics. Wang *et al.*<sup>[31]</sup> modified the commercial high-density polyethylene (HDPE) film with benzylic trimethyl ammonium cations *via* radical graft method. Jeon *et al.*<sup>[32]</sup> grafted a commercial polyethylene (SEBS, polystyrene-*b*-poly(ethylene-co-butylene)-*b*-polystyrene) with alkyl trimethyl ammonium cations. The prepared AEMs showed no loss in conductivity over 500 h in 1 M NaOH at 80 °C. Note that polyethylene AEMs typically

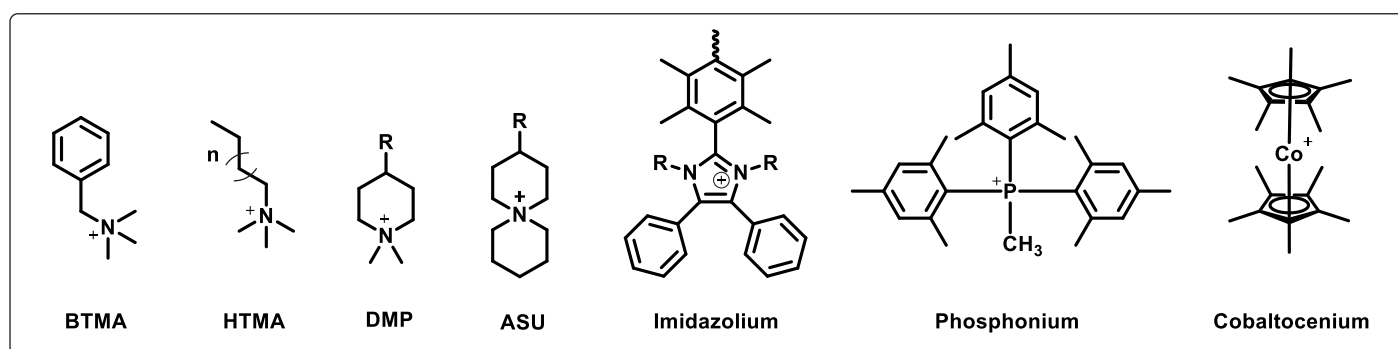


Fig. 4. Typical cations used in AEMs.

exhibit high water uptake and dimensional swelling due to their flexible chains and low glass transition temperature ( $T_g < 100\text{ }^\circ\text{C}$ ).

Polynorbornenes were initially reported by Clark *et al.*<sup>[33]</sup> in 2009 as backbones to prepare AEMs *via* ring-opening metathesis polymerization (ROMP). Recently, Mamdal *et al.*<sup>[34]</sup> developed a new type of polynorbornene AEM through vinyl addition polymerization, which showed no conductivity loss after 1200 h immersion in 1 M KOH at  $80\text{ }^\circ\text{C}$ . This is due to the additional conformation constraints and absence of C=C bonds in the polymer structure. Using this AEM in a fuel cell test, Hassan *et al.*<sup>[35]</sup> achieved a peak power density of  $3200\text{ mW cm}^{-2}$  by carefully manipulating water management. Despite the advantages of polynorbornene AEMs, the complex synthesis process and reliance on precious metal catalysts (Ru or Pd) are their drawbacks.

Ether-free polyaromatics possess many desirable properties, including good thermal, dimensional and mechanical stabilities, as well as excellent chemical stability resulting from the high glass transition temperature and the absence of ether groups. Several synthesis methods have been developed to produce ether-free polyaromatics.

Poly(phenylene)s<sup>[36–38]</sup> made by Diels-Alders polymerization were one of the earliest examples. The polymers were subsequently modified with alkyl halide groups, followed by a quaternarization reaction to prepare AEMs. Poly(phenylene)s AEMs displayed a conductivity of  $119\text{ mS cm}^{-1}$  at  $80\text{ }^\circ\text{C}$  and demonstrated no IEC loss after 670 h in 4 M NaOH at  $60\text{ }^\circ\text{C}$ . One main obstacle of poly(phenylene)s is the multi-step synthesis of both monomers and polymers.

Palladium-catalyzed Suzuki coupling reaction and nickel-catalyzed cross-coupling reactions are efficient methods to synthesize ether-free polyaromatics. Lee *et al.*<sup>[39]</sup> reported a poly(flourene-benzene) (PFB) *via* Suzuki coupling reaction, using aromatics boronic acid/boronated esters and aromatic bromide with a palladium complex. Ono *et al.*<sup>[40]</sup> designed a poly(perfluoroalkylene phenylene) *via* nickel-catalyzed coupling reaction, using dichlorobenzene and perfluoroalkylene with nickel complex. AEMs derived from these backbones showed high chemical stability with no conductivity loss over 1000 h in 1 M KOH at  $80\text{ }^\circ\text{C}$ . However, there are some drawbacks. The Suzuki coupling reaction has limited scalability due to costly palladium catalysts and boronated monomers. Nickel-catalyzed coupling reaction requires large excessive amounts of nickel catalysts for high molecular weight polymers and the removal of nickel metal may bring extra cost.

Super-acid catalyzed Friedel-Crafts reaction is another method to prepare ether-free polyaromatics by forming C-C bonds between ketones and phenyl monomers. This approach allows for the synthesis of diverse polyaromatic structures based on the

choice of electrophilic ketone and phenyl monomers. Lee *et al.*<sup>[41]</sup> reported poly(phenyl alkylene)s with flexible alkyl bromide side chains, which were subsequently converted into ammonium cations. Olsson *et al.*<sup>[20]</sup> synthesized poly(aryl piperidinium)s using commercial N-methyl-4-piperidone monomers. The prepared AEMs exhibited exceptional chemical stability. Furthermore, this reaction is a one-step process, metal-free and easy to scale-up.

### 3.3 Trade-off

#### 3.3.1 Crosslinking

A high IEC ( $>2\text{ meq g}^{-1}$ ) is required to achieve sufficient conductivity in anion exchange membranes (AEMs). However, this often leads to increased water uptake and swelling, resulting in poor mechanical properties. Crosslinking (Fig. 6)<sup>[42]</sup> is an effective method to address this trade-off limitation. The poly(butyl norbornene-b-bromobutyl norbornene-b-butyl norbornene-b-bromobutyl norbornene) AEM with  $3.84\text{ meq g}^{-1}$  IEC adsorbed a huge amount of water. Mandal *et al.*<sup>[15]</sup> used N,N,N',N'-tetramethyl-1,6-hexanediamine (TMHDA) as a crosslinker and observed significant improvements even with a small amount of crosslinking. The AEM with 5% crosslinker exhibited slightly lower IEC ( $3.76\text{ meq g}^{-1}$  vs  $3.84\text{ meq g}^{-1}$ ), but maintained constant conductivity while reducing water uptake dramatically to 122%. Another example by You *et al.*<sup>[43]</sup> involved the crosslinking of polyethylene AEMs. The crosslinked AEM with 10% crosslinker exhibited lower water uptake (115%) and swelling ratio (17%) compared to the pristine AEM (water uptake: 257%, swelling ratio: 46%). Crosslinking is a versatile method to address the trade-off limitation in AEMs, but it also brings difficulties in membrane casting due to the insolubility of crosslinked polymers in many solvents.<sup>[42,44]</sup>

#### 3.3.2 Phase Separation

Creating a microphase separation morphology in AEMs is a strategy inspired by the structure of Nafion membrane to address the trade-off limitation.<sup>[45]</sup> The interconnected hydrophilic channels in Nafion membrane facilitate the rapid migration of protons, and a similar mechanism can be utilized for  $\text{OH}^-$  ion transport. Li *et al.*<sup>[46]</sup> observed that block poly(flourene alkylene) AEM, compared to random poly(flourene alkylene) AEM, exhibited higher conductivity ( $207.9$  vs  $144.1\text{ mS cm}^{-1}$ ) and lower water uptake ( $72.9\%$  vs  $99.3\%$ ) despite having the same IEC ( $2\text{ meq g}^{-1}$ ). They attributed this to the presence of long-range hydrophobic segments and hydrophilic ion clusters in the block poly(flourene alkylene) AEM, which were absent in the random poly(flourene alkylene) AEM (Fig. 7).

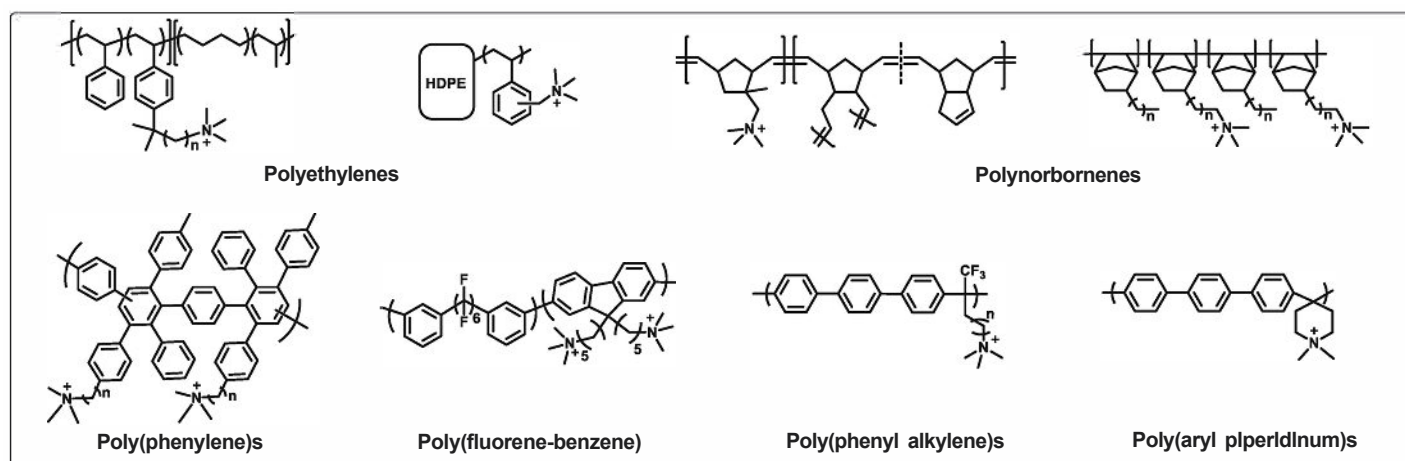


Fig. 5. Aryl-ether free polyaromatics AEMs.



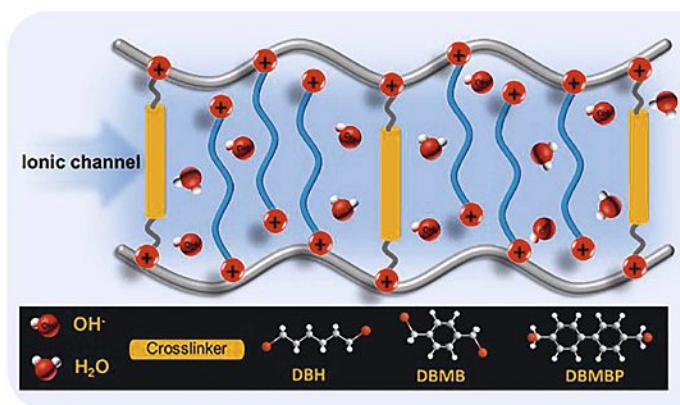


Fig. 6. Illustration of crosslinked AEMs.

#### 4. Poly (aryl piperidinium)s

Extensive research has focused on developing AEMs to address conductivity, chemical stability and trade-off limitations. Among them, poly(aryl piperidinium) (PAP) has emerged as a promising candidate due to its ease of synthesis and scalability. PAP-based AEMs have exhibited exceptional stability in 1 M KOH at 80 °C for over 5000 h. However, the trade-off between ion conductivity and dimensional stability remains a challenge. Olsson *et al.*<sup>[20]</sup> reported the high water uptake (> 145% at 20 °C) of the poly(p-terphenyl N,N-dimethyl piperidinium) (PTPipQ1) membrane, due to its high IEC (2.8 meq. g<sup>-1</sup>) and low molecular weight. To overcome this limitation, various strategies, including copolymerization, crosslinking, branching and microphase separation (Fig. 8), have been developed to enhance PAP-based AEMs, and some are being commercialized by companies such as Versogen (US), W-SCOPE (South Korea), and NovaMea SA (Switzerland).

##### 4.1 Copolymerized PAP AEMs

Several strategies, including copolymerization, crosslinking and phase separation, have been developed to address this trade-off limitation of PAP AEMs. Copolymerization with highly reactive monomers results in polymers with high molecular weight and adjustable IEC, while maintaining the high chemical stability of piperidinium cation and backbones. AEMs based on these high-molecular-weight PAPs exhibit improved OH<sup>-</sup> conductivity and dimensional stability. Wang *et al.*<sup>[47]</sup> demonstrated this by synthesizing PAP-TP-85 through copolymerization with 2,2,2-trifluoroacetophenone monomer, resulting in a polymer with double the intrinsic viscosity of pristine PTP (4.71 dL g<sup>-1</sup> vs. 2.84 dL g<sup>-1</sup>). The PAP-TP-85 AEM displayed high conductivity (170 mS cm<sup>-1</sup> at 80 °C) and excellent dimensional stability (57% water uptake and 10% swelling ratio). The AEMFCs with PAP-TP-85 AEM

achieved a peak power density of 920 mW cm<sup>-2</sup> and durability of 300 h. Chen *et al.*<sup>[48,49]</sup> discovered another two reactive monomers (1,2-diphenylethane and 9,9'-dimethylfluorene) and the prepared PDTP and PFTP AEMs exhibited desirable properties and excellent AEMFCs performances.

##### 4.2 Microphase-separated PAP AEMs

Improving the microphase separation has been recognized as an efficient strategy to address the trade-off in aryl-ether polyaromatics AEMs. However, constructing microphase-separated structures in poly(aryl piperidinium)s AEMs is challenging due to the direct attachment of piperidinium cations to hydrocarbon backbones. Only few poly(aryl piperidinium)s have been reported with improved microphase separation.<sup>[50]</sup> Pham *et al.*<sup>[51]</sup> synthesized a side-chain type poly(terphenyl) with piperidinium cations connected along the backbone *via* a flexible alkylene spacer, leading to the formation of ionic clustering. Another example is the grafting of multiple trimethylammonium groups onto piperidinium rings to create multi-cation side-chain poly(aryl piperidinium) AEMs. Atomic force microscopy (AFM) revealed the presence of larger hydrophilic channels (16.5–18.5 nm) in these AEMs.<sup>[52]</sup>

Recently, our group reported a fluorination strategy to induce phase-separated structures in PAP AEMs.<sup>[53]</sup> We synthesized a series of fluoroalkyl monomers and incorporated them into poly(aryl piperidinium)s, resulting in fluorinated poly(aryl piperidinium)s (FPAP). The high hydrophobicity of the fluoroalkyl chains facilitated the aggregation of piperidinium cations into interconnected hydrophilic channels. The resulting FPAP AEMs exhibited high OH<sup>-</sup> conductivity (>150 mS cm<sup>-1</sup> at 80 °C) and excellent dimensional stability (swelling ratio <20% at 80 °C), comparable to the benchmark Nafion membrane. Furthermore, the FPAP AEMs demonstrated exceptional mechanical properties (tensile strength >80 MPa and elongation at break >40%) and chemical stability (>2000 h in 3 M KOH at 80 °C). Notably, AEMFCs with a FPAP AEM and PGM-free (Co-Mn spinel) cathode achieved a state-of-the-art peak power density of 1.3 W cm<sup>-2</sup> at 80 °C. The FPAP membranes exhibited operational stability for over 500 h.

##### 4.3 Crosslinked PAP AEMs

Crosslinking offers a general approach to mitigate the trade-off between conductivity and dimensional stability in poly(aryl piperidinium) membranes. One method involves reacting with dibromo crosslinkers, as demonstrated by Chen *et al.*<sup>[54]</sup> using a 1,5-dibromopentane crosslinker to create x-PFTP-10 AEMs with 10% crosslinking. These membranes exhibited lower water uptake, reduced swelling ratio, and higher mechanical strength compared to pristine membranes. However, the OH<sup>-</sup> conductivity of the crosslinked membranes was slightly decreased. To address this, the same group<sup>[52]</sup> developed multi-cation crosslinked poly(aryl piperidinium) membranes, which showed improved OH<sup>-</sup> conductivity (155 mS cm<sup>-1</sup> at 80 °C) compared to pristine membranes (102 mS cm<sup>-1</sup> at 80 °C). However, the crosslinked PAP membranes experienced around 10% conductivity loss over 1200 h in 1 M NaOH at 80 °C, likely attributed to the Hoffmann elimination degradation of the crosslinkers.

##### 4.4 Branched PAP AEMs

Recently, our group<sup>[55]</sup> developed a facile synthetic approach to branched poly(aryl piperidinium) AEMs using 1,3,5-triphenyl benzene as branching agent. The resulting branched PAP polymers exhibited high OH<sup>-</sup> conductivity (>145 mS cm<sup>-1</sup> at 80 °C), reduced water uptake and swelling ratio, and favorable mechanical properties (tensile strength >60 MPa and elongation at break >35%). These improvements were attributed to enhanced chain rigidity and increased polymer molecular weight. The membrane maintained its integrity and conductivity after immersion in 1M KOH for 1500 h at 80 °C. AEMFCs based on this membrane

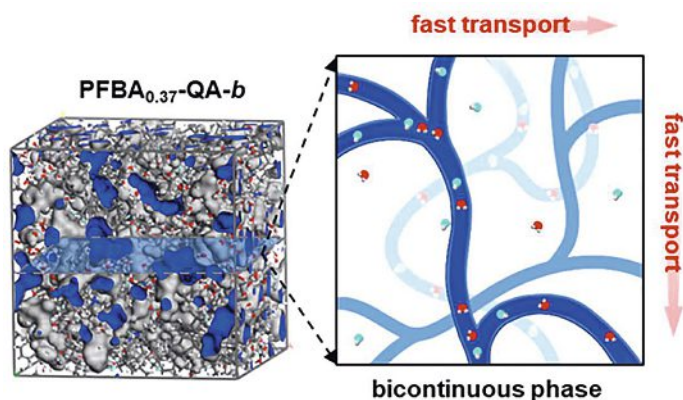


Fig. 7. The molecular dynamics simulation of OH<sup>-</sup> transport through hydrophilic channels in block AEMs.

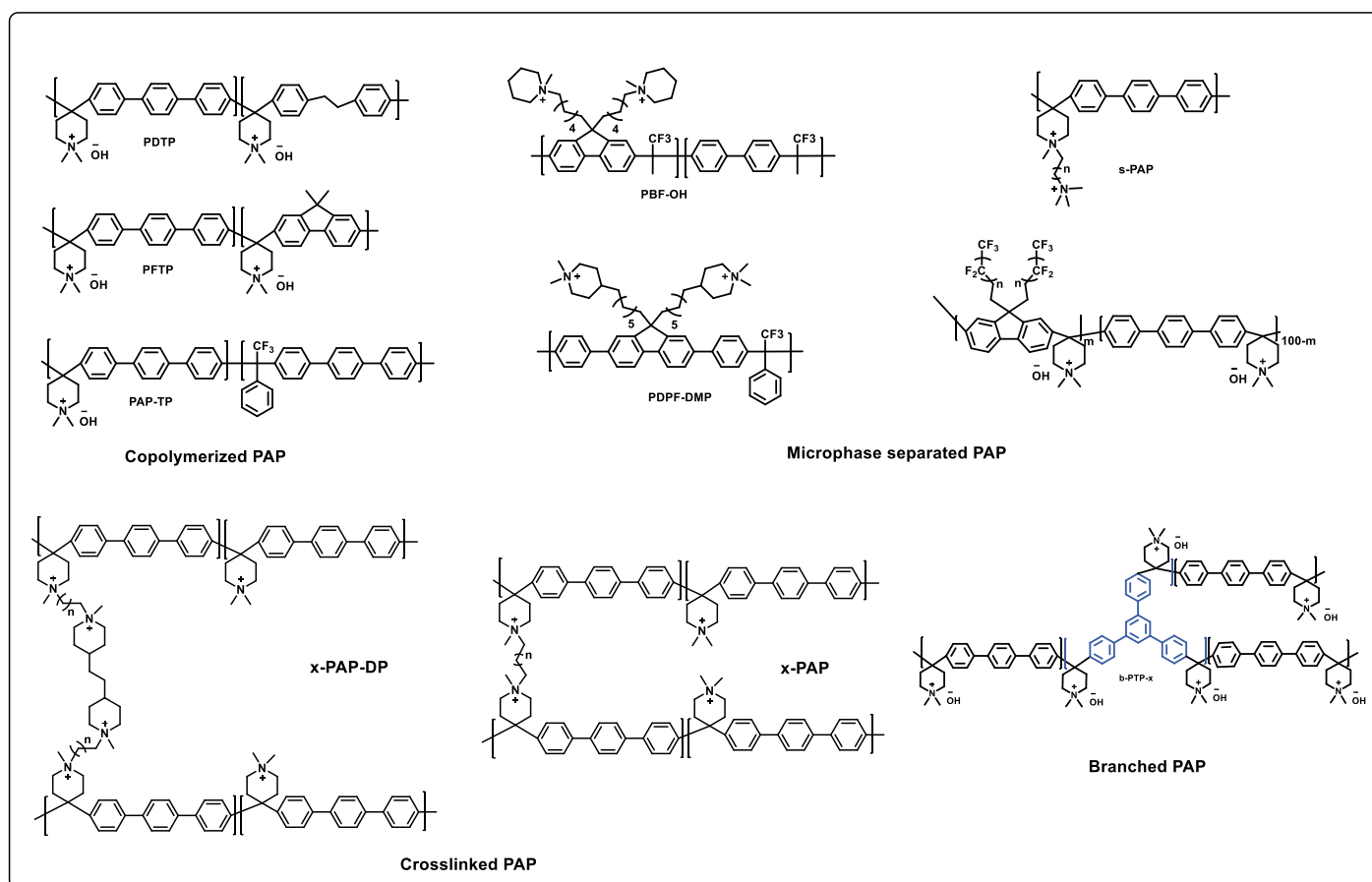


Fig. 8. Chemical structures of copolymerized, microphase separated, crosslinked and branched PAPs.

achieved impressive peak power densities (PPDs) of up to  $2.3 \text{ W cm}^{-2}$  in  $\text{H}_2\text{-O}_2$  and up to  $1.3 \text{ W cm}^{-2}$  in  $\text{H}_2\text{-air}$ , which are among the highest reported values for AEMFCs. The AEMFCs exhibited stable operation for over 500 h, with the branched PAP membrane remaining structurally stable throughout the process. Li *et al.*<sup>[56]</sup> further demonstrated this strategy in branched poly(arylene alkylene) AEMs. The strategy of branching might be applicable to the development of other types of AEMs.

## 5. Summary and Outlook

At the beginning of this review, we highlighted three major challenges hindering the development of AEMs. However, over the past decade, we have witnessed significant scientific advancements in AEMs, leading to the development of various promising materials. Among them, poly(aryl piperidinium)s AEMs have emerged as particularly promising candidates for applications, garnering extensive research attention. Indeed several startup companies have been founded to commercialize these AEMs. Among them is NovaMea SA (novamea-tech.com), a spin-off from our EPFL lab. NovaMea aims to develop next-generation AEM water electrolyzers and fuel cells.

In the future, further improvement in the mechanical durability of poly(aryl piperidinium)s AEMs is crucial because thin membranes ( $<20 \mu\text{m}$ ) are required in fuel cells. Strategies such as incorporating fillers into the polymer matrix and composite with commercial substrates offer potential solutions for enhancing mechanical robustness.

## Acknowledgements

Our work in this area is supported by EPFL.

- [1] European Commission, 'The 2030 Climate Target Plan', <https://eur-lex.europa.eu/legal-content/EN/TXT/PDF/?uri=CELEX:52020DC0562>, Brussels, Sept. 17, 2020.
- [2] P. Jaramillo, S. K. Ribeiro, P. Newman, S. Dhar, O. E. Diemuodeke, T. Klajino, D. S. Lee, S. B. Nugroho, X. Ou, A. H. Stromman, J. Whitehead, 'Climate Change 2022: Mitigation of Climate changes', 2022, Transport, IPCC.
- [3] D. A. Cullen, K. C. Neyerlin, R. K. Ahluwalia, R. Mukundan, K. L. More, R. L. Borup, A. Z. Weber, D. J. Myers, A. Kusoglu, *Nat. Energy* **2021**, 6, 462, <https://doi.org/10.1038/s41560-021-00775-z>.
- [4] 'Fuel Cells and Hydrogen Joint Undertaking', in 'Hydrogen Roadmap Europe', <https://www.fch.europa.eu/>, 2019.
- [5] K. A. Mauritz, R. B. Moore, *Chem. Rev.* **2004**, 104, 10, 4535, <https://doi.org/10.1021/cr0207123>.
- [6] J. Peron, A. Mani, X. Zhao, D. Edwards, M. Adachi, T. Soboleva, Z. Shi, Z. Xie, T. Navessin, S. Holdcroft, *J. Membrane Sci.* **2010**, 356, 44, <https://doi.org/10.1016/j.memsci.2010.03.025>.
- [7] H. L. Salerno, F. L. Beyer, Y. A. Elabd, *J. Poly. Sci. B: Poly. Phys.* **2012**, 50, 8, 552, <https://doi.org/10.1002/polb.23033>.
- [8] S. Lee, H. Lee, T. H. Yang, B. Bae, N. A. T. Tran, Y. Cho, N. Jung, D. Shin, *Membranes* **2020**, 10, 11, 306, <https://doi.org/10.3390/membranes10110306>.
- [9] W. E. Mustain, M. Chatenet, M. Page, Y. S. Kim, *Ener. Environ. Sci.* **2020**, 13, 2805, <https://doi.org/10.1039/D0EE01133A>.
- [10] J. Parrondo, S. Wang, M. S. J. Jung, V. Raman, *Phys. Chem. Chem. Phys.* **2016**, 18, 19705, <https://doi.org/10.1039/C6CP01978A>.
- [11] T. Nemeth, T. Nausser, L. Gubler, *ChemSusChem* **2022**, 15, e202201571, <https://doi.org/10.1002/cssc.202201571>.
- [12] J. Pan, L. Zhu, J. Han, M. A. Hickner, *Chem. Mater.* **2015**, 27, 19, 6689, <https://doi.org/10.1021/acs.chemmater.5b02557>.
- [13] B. Lin, F. Xu, Y. Su, J. Han, Z. Zhu, F. Chu, Y. Ren, L. Zhu, J. Ding, *ACS Appl. Ener. Mater.* **2019**, 3, 1, 1089, <https://doi.org/10.1021/acs.energmat.9b02123>.
- [14] Y. He, J. Pan, L. Wu, Y. Zhu, X. Ge, J. Ran, Z. Yang, T. Xu, *Sci. Rep.* **2015**, 5, 13417, <https://doi.org/10.1038/srep13417>.
- [15] M. Mandal, G. Huang, N. U. Hassan, X. Peng, T. Gu, A. H. Brooks-Starks, B. Bahar, W. E. Mustain, P. A. Kohl, *J. Electrochem Soc.* **2020**, 167, 054501, <https://doi.org/10.1149/2.0022005JES>.
- [16] H. Peng, Q. Li, M. Hu, L. Xiao, J. Lu, L. Zhuang, *J. Power Sources* **2018**, 390, 165, <https://doi.org/10.1016/j.jpowsour.2018.04.047>.

- [17] M. Marino, K. Kreuer, *ChemSusChem* **2015**, *8*, 3, 513, <https://doi.org/10.1002/cssc.201403022>.
- [18] M. K. Hugar, W. You, G. W. Coates, *ACS Ener. Lett.* **2019**, *4*, 7, 1681, <https://doi.org/10.1021/acsenerylett.9b00908>.
- [19] J. S. Olsson, T. H. Pham, P. Jannasch, *Macromolecules* **2017**, *50*, 7, 2783, <https://doi.org/10.1021/acs.macromol.7b00168>.
- [20] J. S. Olsson, T. H. Pham, P. Jannasch, *Adv. Funct. Mater.* **2018**, *28*, 2, 1702758, <https://doi.org/10.1002/adfm.201702758>.
- [21] Y. Ye, K. K. Stokes, F. L. Beyer, Y. A. Elabd, *J. Membrane Sci.* **2013**, *443*, 93, <https://doi.org/10.1016/j.memsci.2013.04.053>.
- [22] S. Gu, R. Cai, T. Luo, Z. Chen, M. Sun, Y. Liu, G. He, Y. Yan, *Angew. Chem. Int. Ed.* **2009**, *121*, 35, 6621, <https://doi.org/10.1002/ange.200806299>.
- [23] S. Gu, R. Cai, T. Luo, K. Jensen, C. Contreras, Y. Yan, *ChemSusChem* **2010**, *3*, 555, <https://doi.org/10.1002/cssc.201000074>.
- [24] N. Chen, H. Zhu, Y. Chu, R. Li, Y. Liu, F. Wang, *Polym. Chem.* **2017**, *8*, 1381, <https://doi.org/10.1039/C6PY01936F>.
- [25] T. Zhu, Y. Sha, H. A. Firouzjaie, X. Peng, Y. Cha, D. M. Dissanayake, M. D. Smith, *J. Am. Chem. Soc.* **2019**, *142*, 2, 1083, <https://doi.org/10.1021/jacs.9b12051>.
- [26] B. Zhang, S. Gu, J. Wang, L. Li, A. M. Herring, Y. Yan, *RSC Adv.* **2012**, *2*, 12683, <https://doi.org/10.1039/C2RA21402D>.
- [27] X. Ge, Y. He, M. D. Guiver, L. Wu, J. Ran, Z. Yang, T. Xu, *Adv. Mater.* **2016**, *28*, 18, 3467, <https://doi.org/10.1002/adma.201506199>.
- [28] J. Chen, C. Li, J. Wang, L. Li, Z. Wei, *J. Mater. Chem. A* **2017**, *5*, 6318, <https://doi.org/10.1039/C7TA00879A>.
- [29] X. Chu, Y. Shi, L. Liu, Y. Huang, N. Li, *J. Mater. Chem. A* **2019**, *7*, 7717, <https://doi.org/10.1039/C9TA01167F>.
- [30] C. G. Arges, V. Ramani, *Proc. Natl. Acad. Sci. USA* **2013**, *110*, 7, 2490, <https://doi.org/10.1073/pnas.1217215110>.
- [31] L. Wang, X. Peng, W. E. Mustain, J. R. Varcoe, *Ener. Environ. Sci.* **2019**, *12*, 1575, <https://doi.org/10.1039/C9EE00331B>.
- [32] J. Y. Jeon, S. Park, J. Han, S. Maurya, A. D. Mohanty, D. Tian, N. Saikia, M. A. Hickner, C. Y. Ryu, M. E. Tuckerman, *Macromolecules* **2019**, *52*, 5, 2139, <https://doi.org/10.1021/acs.macromol.8b02355>.
- [33] T. J. Clark, N. J. Robertson, H. A. Kostalik IV, E. B. Lobkovsky, P. F. Mutolo, H. D. Abruna, G. W. Coates, *J. Am. Chem. Soc.* **2009**, *131*, 36, 12888, <https://doi.org/10.1021/ja905242r>.
- [34] M. Mandal, G. Huang, P. A. Kohl, *J. Membrane Sci.* **2019**, *570-571*, 394, <https://doi.org/10.1016/j.memsci.2018.10.041>.
- [35] N. Ul Hassan, M. Mandal, G. Huang, H. A. Firouzjaie, P. A. Kohl, W. E. Mustain, *Adv. Ener. Mater.* **2020**, *10*, 40, 2001986, <https://doi.org/10.1002/aenm.202001986>.
- [36] D. Li, E. J. Park, W. Zhu, Q. Shi, Y. Zhou, H. Tian, Y. Lin, A. Serov, B. Zulevi, E. D. Baca, *Nat. Energy* **2020**, *5*, 378, <https://doi.org/10.1038/s41560-020-0577-x>.
- [37] M. R. Hibbs, C. H. Fujimoto, C. J. Cornelius, *Macromolecules* **2009**, *42*, 21, 8316, <https://doi.org/10.1021/ma901538c>.
- [38] E. J. Park, S. Maurya, M. R. Hibbs, C. H. Fujimoto, K. D. Kreuer, Y. S. Kim, *Macromolecules* **2019**, *52*, 14, 5419, <https://doi.org/10.1021/acs.macromol.9b00853>.
- [39] W. H. Lee, A. D. Mohanty, C. Bae, *ACS Macro Lett.* **2015**, *4*, 4, 453, <https://doi.org/10.1021/acsmacrolett.5b00145>.
- [40] H. Ono, J. Miyake, S. Shimada, M. Uchida, K. Miyatake, *J. Mater. Chem. A* **2015**, *3*, 21779, <https://doi.org/10.1039/C5TA06454F>.
- [41] W. H. Lee, Y. S. Kim, C. Bae, *ACS Macro Lett.* **2015**, *4*, 814, <https://doi.org/10.1021/acsmacrolett.5b00375>.
- [42] C. Hu, X. Deng, X. Dong, Y. Hong, Q. Zhang, Q. Liu, *J. Membrane Sci.* **2021**, *619*, 118806, <https://doi.org/10.1016/j.memsci.2020.118806>.
- [43] W. You, E. Padgett, S. N. MacMillan, D. A. Muller, G. W. Coates, *Proc. Natl. Acad. Sci. USA* **2019**, *116*, 20, 9729, <https://doi.org/10.1073/pnas.1900988116>.
- [44] S. Pal, R. Mondal, S. Guha, U. Chatterjee, S. K. Jewrajka, *J. Membrane Sci.* **2020**, *612*, 118459, <https://doi.org/10.1016/j.memsci.2020.118459>.
- [45] A. Lehmani, P. Turq, M. Périé, J. Périé, J. P. Simonin, *J. Electroanal. Chem.* **1997**, *428*, 81, [https://doi.org/10.1016/S0022-0728\(96\)05060-7](https://doi.org/10.1016/S0022-0728(96)05060-7).
- [46] X. Li, K. Yang, Z. Wang, Y. Chen, Y. Li, J. Guo, J. Zheng, S. Li, S. Zhang, *Macromolecules* **2022**, *53*, 23, 10607, <https://doi.org/10.1021/acs.macromol.2c01488>.
- [47] J. Wang, Y. Zhao, B. P. Setzler, S. Rojas-Carbonell, C. B. Yehuda, A. Amel, M. Page, L. Wang, K. Hu, L. Shi, S. Gottesfeld, B. Xu, Y. Yan, *Nat. Energy* **2019**, *4*, 392, <https://doi.org/10.1038/s41560-019-0372-8>.
- [48] N. Chen, H. H. Wang, S. P. Kim, H. M. Kim, W. H. Lee, C. Hu, J. Y. Bae, E. S. Sim, Y. C. Chung, J. H. Jang, S. J. Yoo, Y. Zhuang, Y. M. Lee, *Nat. Commun.* **2021**, *12*, 2367, <https://doi.org/10.1038/s41467-021-22612-3>.
- [49] N. Chen, C. Hu, H. H. Wang, S. P. Kim, H. M. Kim, W. H. Lee, J. Y. Bae, J. H. Park, Y. M. Lee, *Angew. Chem. Int. Ed.* **2021**, *60*, 7710, <https://doi.org/10.1002/anie.202013395>.
- [50] T. H. Pham, A. Allushi, J. S. Olsson, P. Jannasch, *Polym. Chem.* **2020**, *11*, 6953, <https://doi.org/10.1039/D0PY01291B>.
- [51] T. H. Pham, J. S. Olsson, P. Jannasch, *J. Mater. Chem. A* **2019**, *7*, 15895, <https://doi.org/10.1039/C9TA05531B>.
- [52] H. M. Kim, C. Hu, H. H. Wang, J. H. Park, N. Chen, Y. M. Lee, *J. Membrane Sci.* **2022**, *644*, 120109, <https://doi.org/10.1016/j.memsci.2021.120109>.
- [53] X. Wu, N. Chen, C. Hu, H. A. Klok, Y. M. Lee, X. Hu, *Adv. Mater.* **2023**, *2210432*, <https://doi.org/10.1002/adma.202210432>.
- [54] N. Chen, J. H. Park, C. Hu, H. H. Wang, H. M. Kim, N. Y. Kang, Y. M. Lee, *J. Mater. Chem. A* **2022**, *10*, 3678, <https://doi.org/10.1039/D1TA10178A>.
- [55] X. Wu, N. Chen, H. A. Klok, Y. M. Lee, X. Hu, *Angew. Chem. Int. Ed.* **2022**, *61*, 7, e202114892, <https://doi.org/10.1002/anie.202114892>.
- [56] L. Li, T. Jiang, S. Wang, S. Cheng, X. Li, H. Wei, Y. Ding, *ACS Appl. Ener. Mater.* **2022**, *5*, 2, 2462, <https://doi.org/10.1021/acsaem.1c03952>.

#### License and Terms



This is an Open Access article under the terms of the Creative Commons Attribution License CC BY 4.0. The material may not be used for commercial purposes.

The license is subject to the CHIMIA terms and conditions: (<https://chimia.ch/chimia/about>).

The definitive version of this article is the electronic one that can be found at <https://doi.org/10.2533/chimia.2023.494>